

DESIGN METHOD OF MINIATURIZED RING COUPLER USING PHASE SHIFTERS CONSISTING OF FULLY-DISTRIBUTED COMPOSITE RIGHT/LEFT-HANDED STRUCTURES

Stefan Simion*

Department of Electronics and Communications of Military Technical Academy, George Cosbuc 39-49, Bucharest 050141, Romania

Abstract—A new method to design a miniaturized ring coupler consisting of multiple open stubs on the inside of the ring is proposed. It is shown that this coupler topology may be seen as fully-distributed composite right/left handed (CRLH) small-size phase shifters, cascaded in a ring configuration. The CRLH phase shifter is analyzed in detail and a design method is proposed, pointing out the condition to obtain a reduction of its length. Using the fully-distributed CRLH based phase shifter, a ring coupler is configured and analyzed in comparison with the traditional ring coupler, showing that both couplers have similar characteristics. To validate the proposed design method, a 3-dB CRLH based ring coupler is designed and fabricated. The experimental results show a very good agreement with the predicted results obtained by electromagnetic simulation. The printed area of the fabricated coupler is 49% smaller compared to the traditional ring coupler.

1. INTRODUCTION

The hybrid ring directional coupler is one of the most used microwave devices, in applications such as mixers, modulators, push-pull amplifiers and array antennas circuitry. Since the traditional ring coupler consisting of a ring of 1.5λ circumference was proposed more than 50 years ago [1], other semi-lumped or fully-distributed configurations of ring couplers have been developed to reduce the circuit printed area [2–11], to extend the frequency bandwidth [4–6, 12, 13], or to obtain dual-band frequency response [14].

Received 10 February 2013, Accepted 25 March 2013, Scheduled 28 March 2013

* Corresponding author: Stefan Simion (stefan.simion@yahoo.com).

In particular, referring to the ring coupler miniaturization, instead of using $\lambda/4$ line sections, shorter line sections of $\lambda/6$ or $\lambda/8$ length can be used, this way the circumference of the ring coupler may be reduced from 1.5λ to 1.25λ or $7\lambda/6$ [2]. Also, using shorter line sections to realize the coupler ring, design formulas to reduce the ring circumference to $15\lambda/14$ are given in [3]. The coupler parameters reported in [2, 3] are similar to the traditional ring coupler.

Another solution to reduce the coupler printed area is to use a coplanar strip crossover based 180° phase inverter, in order to reduce the length of the $3\lambda/4$ line section to $\lambda/4$ as for the other three line sections of the traditional ring coupler [4–6]. With this technique, the frequency bandwidth may be increased by 28% compared to the traditional ring coupler, with a return-loss greater than 20 dB [6]. Unfortunately, this design solution cannot be implemented with microstrip lines and, moreover, bonding wires are needed.

Using phase shifters consisting of semi-lumped composite right/left-handed (CRLH) structures, the coupler printed area may be reduced, up to 56% and 67%, as reported in [7, 8], respectively (in [8], a significant bandwidth enhancement has been also attained). In spite of the size reduction, due to the using of lumped elements, the design for these coupler topologies is not very easy. It involves the modeling of lumped components, the layout design which must take into account the parasitic effects due to the soldering of lumped components, but also additional technological processes are needed compared to those applied for a fully-distributed topology.

Fully-distributed miniaturized ring coupler using CRLH based microstrip coupled-line structures has been reported in [9], where the area reduction up to 60% has been obtained. For this solution, the frequency bandwidth is about 80% compared to the traditional ring coupler, but, on the other hand, it may be fabricated easily using one mask technological process. Another fully-distributed configuration having practically the same characteristics as the traditional ring coupler, also easily implemented with microstrip lines, has been reported in [10]. It consists of multiple open stubs on the inside of the ring. It is shown that a $\lambda/4$ line section may be replaced by cascading a number of equivalent units, each one made up of a main transmission line with two shunted open stubs. The shorter the equivalent unit is, the greater the number of units is. Formulas are given for the equivalence between the line section and the equivalent unit, obtaining the same characteristic impedances for all the open stubs which have the same electrical lengths chosen arbitrarily. It is shown that for one unit, the open stubs characteristic impedance is very low from practical point of view. On the other hand, practical value

for the open stubs characteristic impedance may be obtained for three cascaded units, but the open stubs are too close to each other and the resulting coupling effects may affect the coupler characteristics. Also, the characteristic impedance of the main transmission line increases to unpractical values. For two units, practical values for the characteristic impedance of the transmission lines are obtained, but no analysis regarding the optimum electrical lengths for the open stubs is provided.

In [11], it is shown briefly that this coupler topology may be seen as consisting of fully-distributed CRLH based phase shifters. In the present paper, it is demonstrated in detail that using the CRLH approach, an accurate design method may be developed and the condition to obtain the area reduction may be pointed out. Moreover, comparing to the design method presented in [10], following the method presented in this paper, the characteristic impedances of the open stubs may have different values. In this way, the technological constrains and the size reduction requirements may be balanced more efficiently.

The paper is organized as follows. In Section 2, the fully-distributed CRLH based phase shifter is analyzed in detail. A design method of this CRLH based phase shifter is also proposed, showing that it is possible to obtain a phase shifter which is shorter, compared to a simple transmission line having the same phase shift at a specified frequency. Using small-size CRLH based phase shifters, in Section 3, CRLH based ring couplers are configured and analyzed. It is shown that this new coupler has similar characteristics as the traditional ring coupler. To validate the design method, a CRLH based ring coupler is fabricated and experimentally characterized. The printed area of the fabricated coupler is 49% smaller compared to the traditional ring coupler topology. In Section 4, the results obtained from measurements are compared to those obtained by electromagnetic simulation, showing that they are in very good agreement.

2. ANALYSIS AND DESIGN OF SMALL-SIZE FULLY-DISTRIBUTED CRLH BASED PHASE SHIFTER

In this section, a design technique based on CRLH approach for modeling a transmission line by a shorter two-port is presented. The starting circuit in this modeling is the fully-distributed CRLH based phase shifter shown in Fig. 1, which will be analyzed in detail in the first part of the section. Because the series stubs may not be implemented in practice using microstrip lines or coplanar waveguides, this circuit may not be fabricated using these planar transmission lines. In the second part of the section, it is shown that this circuit is equivalent with another one which may be implemented practically.

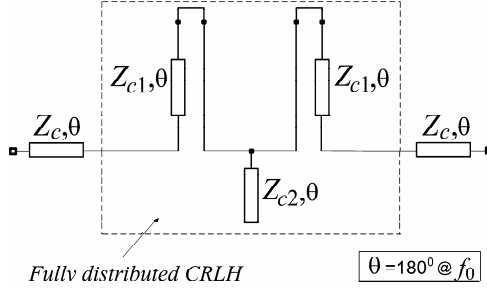


Figure 1. Fully-distributed CRLH based phase shifter, used as a starting circuit toward a small-size phase shifter which may be implemented in practice.

The circuit from Fig. 1 consists of a fully-distributed CRLH structure inserted between two transmission lines of characteristic impedance, Z_c . The short-circuited series stubs of characteristic impedances Z_{c1} and the open-circuited shunt stub of characteristic impedance Z_{c2} are working as series and parallel resonant circuits, respectively, having the same central frequency f_0 , where the electrical lengths of the lines are equal to 180° . In consequence, the fully-distributed CRLH structure shown in Fig. 1 is working as a pass-band filter, around the frequency f_0 (the pass-band responses around frequencies equal to multiple of f_0 are not taken into account). Into the frequency bandwidth of this filter, the phase shift b_{CRLH} and the characteristic impedance $Z_{c,CRLH}$ have real values, and they may be computed using the following formulas, which have been obtained using the general formulas presented in [15] for the k -filter sections:

$$b_{CRLH}(f) = 2 \cdot \sin^{-1} [K(f)] \quad (1)$$

$$Z_{c,CRLH}(f) = Z_c \cdot \sqrt{1 - [K(f)]^2} \quad (2)$$

where

$$Z_c = \sqrt{2Z_{c1}Z_{c2}}, \quad (3)$$

$$K(f) = \frac{Z_c}{2Z_{c2}} \cdot \Omega(f) \quad (4)$$

and

$$\Omega(f) = \tan \left(\pi \frac{f}{f_0} \right). \quad (5)$$

By analyzing the formulas (1), (2), into the frequency bandwidth, the condition $K(f) < 1$ must be fulfilled. Therefore, using (4) and (5), the

cutoff frequencies of the filter may be computed imposing the condition $\frac{Z_c}{2Z_{c2}} \cdot \tan(\pi \frac{f}{f_0}) < 1$.

If the reference impedances at the ports are equal to Z_c , then, the magnitude of S_{11} for this circuit is equal to the magnitude of S_{11} for the fully-distributed CRLH structure. For this reference impedance at both ports, (3) is the perfect impedance matching condition at f_0 , when $Z_{c,CRLH}(f_0)$ is equal to Z_c . Then, for $f = f_0$, $|S_{11}| = 0$ and also $b_{CRLH} = 0$ (see (1), (4) and (5)). For frequencies shifted from f_0 , the expression for the phase shift may be written as:

$$\Phi(f) \cong 2\pi \cdot (f/f_0) + b_{CRLH}(f) \tag{6}$$

where b_{CRLH} is given by (1).

The accuracy of formula (6) is satisfactory for frequencies closed enough to f_0 , when $|S_{11}|$ is small. This impedance matching condition and the imposed value of the phase shift at a specified frequency must be fulfilled together, when the simple transmission line phase shifter is modeled by the circuit given in Fig. 1.

The expression of $|S_{11}|$ for any frequency value may be expressed as

$$|S_{11}| = |K|^3 / \sqrt{1 + K^6} \tag{7}$$

and it is represented graphically in Fig. 2, where K is given by (4). On the same graph, it is shown the variation for the phase shift error per cent, PSE , expressed as

$$PSE = 100 \cdot |(b_{CRLH} + \varphi_{S_{21}}) / b_{CRLH}|, \tag{8}$$

where b_{CRLH} is given by (1) and $\varphi_{S_{21}} = -\tan^{-1}[(2K - K^3)/(1 - 2K^2)]$ is the phase of the S_{21} computed for the fully-distributed CRLH. As

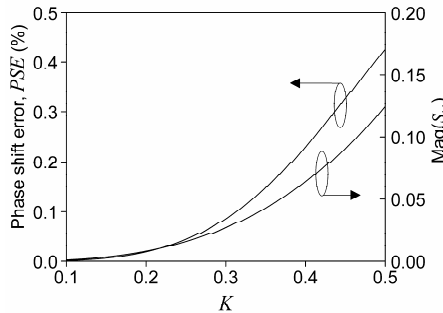


Figure 2. The magnitude of S_{11} and the phase shift error versus K (see (7) and (8), respectively), for the fully-distributed CRLH structure.

much as the value of K decreases, $|S_{11}|$ and PSE decrease, thus the errors made in using formula (6) are smaller and smaller. The error in using (6) is zero for f_0 , when $K = 0$ — see (4) and (5), corresponding to the perfect impedance matching. From (4) and (5), if the frequency shift from f_0 increases, the value of K increases.

Inspecting the circuit from Fig. 1, it is correct to assume that the electrical length of the phase shifter is given by the two transmission lines of characteristic impedance Z_c (it is shown later that the circuit from Fig. 1 is equivalent to another circuit which has the electrical length given by two transmission lines, too).

The scaling factor at a frequency $\Delta f < f_0$ is defined as the ratio between the electrical length of a simple transmission line and the electrical length of the phase shifter shown in Fig. 1, both having the same phase shift, $\Phi(\Delta f)$. By this definition, the scaling factor may be written as:

$$SF = (f_0/\Delta f) \cdot \Phi(\Delta f)/\Phi(f_0) \quad (9)$$

where $\Phi(f_0) = 2\pi$, as it is obtained from (6) for $f = f_0$.

If $SF > 1$, the phase shifter shown in Fig. 1 is shorter than a transmission line having the same phase shift, at the operating frequency Δf .

Using (1), (4) and (5) in (6), for $f = \Delta f$, it is obtained the following equation:

$$\Phi(\Delta f) \cong 2\pi \cdot \frac{\Delta f}{f_0} + 2 \sin^{-1} \left[\frac{Z_c}{2Z_{c2}} \tan \left(\pi \frac{\Delta f}{f_0} \right) \right] \quad (10)$$

Imposing the reference impedance, Z_c and the phase shift $\Phi(\Delta f)$, this equation may be solved for $\Delta f/f_0$, choosing Z_{c2} as parameter.

The phase shifter shown in Fig. 1 may be transformed into an equivalent circuit which may be implemented in practice, if the circuit Kuroda transformation as shown in Fig. 3 is applied [15]. To find the equivalence formulas between the circuits shown in Fig. 3, the transmission matrices of the two circuits must be identical. If the transmission matrix of the left side circuit is denoted $[A]$ and the other circuit is denoted $[B]$, these matrices can be obtained as:

$$[A] = \frac{1}{1 + \Omega^2} \cdot \begin{bmatrix} 1 & j\Omega Z_c \\ \frac{j\Omega}{Z_c} & 1 \end{bmatrix} \cdot \begin{bmatrix} 1 & j\Omega Z_{c1} \\ 0 & 1 \end{bmatrix} \quad (11)$$

and

$$[B] = \frac{1}{1 + \Omega^2} \cdot \begin{bmatrix} 1 & 0 \\ \frac{j\Omega}{2Z'_{c2}} & 1 \end{bmatrix} \cdot \begin{bmatrix} 1 & j\Omega Z'_{c1} \\ \frac{j\Omega}{Z'_{c1}} & 1 \end{bmatrix} \quad (12)$$

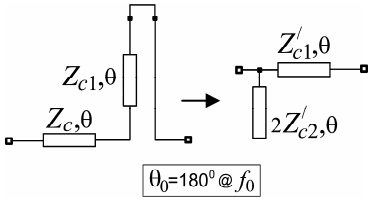


Figure 3. The circuit transformation used to eliminate the series stubs from the phase shifter shown in Fig. 1, in order to obtain a phase shifter which may be implemented in practice.

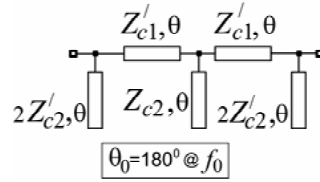


Figure 4. Fully-distributed CRLH based phase shifter which may be easily implemented in practice.

Letting $[A] = [B]$, from (11) and (12), taking into account (3), the following equivalence formulas, valid for any frequency, are obtained:

$$Z'_{c1} = Z_c \cdot \left(1 + \frac{Z_c}{2Z_{c2}} \right) \tag{13}$$

and

$$Z'_{c2} = Z_{c2} + \frac{Z_c}{2} \tag{14}$$

Applying the circuit transformation shown in Fig. 3, the phase shifter based on the fully-distributed CRLH is obtained as given in Fig. 4. This circuit may be easily implemented in practice, by using any type of planar transmission lines.

Imposing $Z_c = 70.7\Omega$ and $\Phi(\Delta f) = 90^\circ$, the computed values for Z'_{c1} , Z'_{c2} (by using the formulas (13) and (14)), $\Delta f/f_0$ (by solving the equation (10)), the K factor (using (4) and (5) for $f = \Delta f$), the scaling factor SF (given by (9)), the return-loss, $RL = -20 \log |S_{11}|$ and PSE at the frequency Δf (using (7) and (8), respectively), are given in Table 1, for different values of Z_{c2} . Analyzing the values given in Table 1, RL increases and PSE decreases, as the values of K decreases (accordingly to Fig. 2, too). Also, the scaling factor SF decreases, as the values of Z_{c2} increases.

For $\Delta f = 1.8\text{GHz}$, the phase shifter given in Fig. 4 has been analyzed using the Microwave Office (MWO) software, for the circuit parameters specified in Table 1. The results obtained for RL have been in very good agreement with the predicted values given in Table 1, the differences between them being within 0.1 dB. Also, for the phase shift $\Phi(\Delta f)$, values between 89.84° and 90.33° have been obtained, very close to the imposed value of 90° . Then, for $\Phi(\Delta f) = 90^\circ$, it is confirmed by circuit simulation that for very small values of PSE ,

Table 1. Parameters of the fully-distributed CRLH based phase shifters, for $\Phi(\Delta f) = 90^\circ$, $Z_c = 70.7 \Omega$ and Z_{c2} from 30Ω to 120Ω .

Z_{c2} (Ω)	Z'_{c1} (Ω)	Z'_{c2} (Ω)	$\frac{\Delta f}{f_0}$	K	SF	RL (dB)	PSE (%)
30	154	65.3	0.110	0.424	2.27	22.3	0.28
40	133.2	75.3	0.128	0.376	1.95	25.6	0.19
50	120.7	85.3	0.141	0.335	1.77	28.5	0.13
60	112.4	95.3	0.152	0.305	1.64	31	0.09
70	106.4	105.3	0.160	0.278	1.56	33.4	0.06
80	101.9	115.3	0.167	0.256	1.50	35.5	0.05
90	98.5	125.3	0.173	0.237	1.44	37.5	0.04
100	95.7	135.3	0.179	0.223	1.40	39.1	0.03
110	93.4	145.3	0.183	0.208	1.37	40.9	0.02
120	91.5	155.3	0.187	0.196	1.34	42.4	0.02

the formula (10) may be used with very small errors for the phase shifter design, for any practical values of Z_{c2} , if Δf and f_0 are chosen accordingly to the ratio $\Delta f/f_0$ given in Table 1.

Taking into account the values of Z'_{c1} and Z'_{c2} , the phase shifters with Z_{c2} between 50Ω and 100Ω may be easier fabricated than the others. For these ones, the electrical length reduction per cent, computed as $100 \cdot (1 - SF^{-1})$, varies from 43% to 28%, compared to the phase shifter consisting of a simple transmission line of electrical length of 90° , at the frequency Δf , having the characteristic impedance equal to 70.7Ω .

For Z_{c2} equal to 50Ω and 100Ω , $\Delta f = 1.8 \text{ GHz}$ ($f_0 = 12.76 \text{ GHz}$ for $Z_{c2} = 50 \Omega$ and $f_0 = 10.05 \text{ GHz}$ for $Z_{c2} = 100 \Omega$), using Z'_{c1} and Z'_{c2} given in Table 1, Fig. 5 shows the magnitude of $|S_{11}|$ and the phase of S_{21} (equal to the phase shift of the phase shifter, but with the opposite sign) versus the frequency, obtained by using MWO. From Fig. 5(a), it is observed that $|S_{11}|$ is the same for Δf and $f_0 \pm \Delta f$, depending on the value of Z_{c2} , according to formula (7) (where (4) and (5) must be taken into account). From Fig. 5(b), the phase shift of S_{21} is -90° at the frequency Δf and $\pm 90^\circ$ at the frequencies $f_0 \pm \Delta f$ (the values of phase shift are reduced to $\pm 180^\circ$). These phase shift values are in very good agreement with the values obtained from (6), as a result of the small values of $|S_{11}|$ at Δf and $f_0 \pm \Delta f$.

Therefore, while a shorter phase shifter may be obtained if the

operating frequency is Δf , the phase shifter may be also used for dual-band applications, at the frequencies pair $f_0 \pm \Delta f$ (the general case for frequency pairs $m f_0 \pm \Delta f$, where m is an integer number greater than 1, it is not of practical interest because of the large area obtained for the phase shifter, but could be of interest for multi-band phase shifters).

In this paper, the design goal is to reduce the phase shifter length, for a single operating frequency (i.e., Δf).

The return-loss at the frequency equal to Δf may be increased, imposing Δf , $\Phi(\Delta f)$ and a minimum value for the return-loss, RL , optimizing the value for the electrical length of the transmission lines

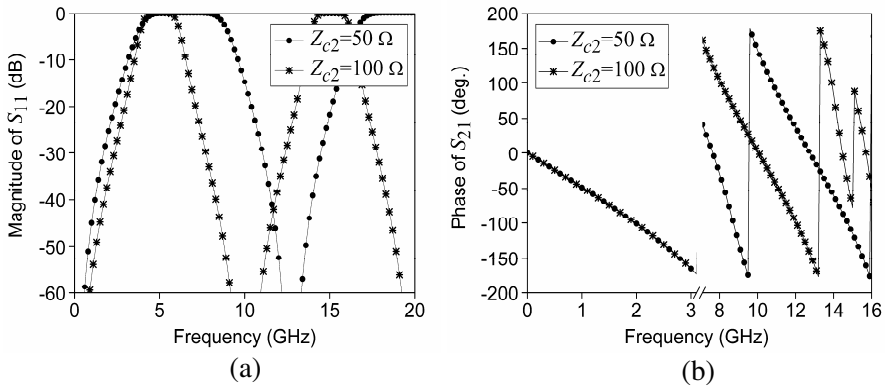


Figure 5. The magnitude of S_{11} and the phase shift of S_{21} for the phase shifter shown in Fig. 4, when Z_{c2} is equal to 50Ω and 100Ω , obtained with MWO (see Table 1 for the other phase shifter parameters).

Table 2. Parameters of the fully-distributed CRLH based phase shifter after the optimization process with MWO, when the return-loss value is imposed to be at least 35 dB at the frequency Δf , for $\Delta f = 1.8 \text{ GHz}$, $\Phi(\Delta f) = 90^\circ$ and $Z_c = 70.7 \Omega$.

$Z_{c2} (\Omega)$	$f_0 (\text{GHz})$	$\Delta\theta (\text{deg}) @ f_0$	SF	$RL (\text{dB})$	$\Phi(\Delta f) (\text{deg})$
50	13.6	18.98	1.71	63.3	90.00
60	12.4	10.68	1.63	42.5	89.42
70	11.52	6.97	1.54	40.8	90.02
80	10.89	3.38	1.48	39.1	90.00
90	10.41	0.92	1.43	38.4	90.04
100	10.07	0.2	1.40	39.4	90.13

Table 3. Parameters of the fully-distributed CRLH based phase shifter after the optimization process with MWO, when the return-loss value is imposed to be of least 50dB at the frequency Δf , for $\Delta f = 1.8$ GHz, $\Phi(\Delta f) = 90^\circ$ and $Z_c = 70.7 \Omega$.

$Z_{c2} (\Omega)$	f_0 (GHz)	$\Delta\theta$ (deg) @ f_0	SF	RL (dB)	$\Phi(\Delta f)$ (deg)
50	13.6	18.98	1.71	63.3	90.00
60	12.5	14.71	1.60	60.7	90.00
70	11.75	12.46	1.53	74	90.00
80	11.14	9.45	1.47	58.3	90.00
90	10.71	8.39	1.42	69.2	90.00
100	10.29	5.48	1.39	51.3	90.00

having the characteristic impedance Z'_{c1} and also the value for the frequency f_0 . After optimization, a greater value for f_0 is obtained and, also, the electrical length of the transmission lines of characteristic impedance Z'_{c1} is extended with $\Delta\theta$, computed at the new value of f_0 .

For $Z_c = 70.7 \Omega$, $\Delta f = 1.8$ GHz and $\Phi(\Delta f) = 90^\circ$, using MWO, the new values for f_0 , SF , RL and $\Phi(\Delta f)$, as well as the values for $\Delta\theta$, are given in Tables 2 and 3, imposing the minimum value of RL at the frequency Δf , equal to 35 dB and 50 dB, respectively, when Z_{c2} varies between 50Ω and 100Ω . The characteristic impedances Z'_{c1} and Z'_{c2} are the same as in the Table 1, therefore they have been omitted. In these tables, it has been used a formula for SF which takes into account the values of $\Delta\theta$ in formula (9), having the expression $SF = (f_0/\Delta f) \cdot \Phi(\Delta f)/[\Phi(f_0) + 2 \cdot \Delta\theta]$, where $\Phi(f_0) = 2\pi$, $\Phi(\Delta f) = \pi/2$ and f_0 is the new value obtained by optimization.

Analyzing the results presented in Tables 2 and 3, it is observed that the values for the scaling factor SF are slightly better for the case when the return-loss is imposed to a minimum value of 35 dB. Also, the phase shift $\Phi(\Delta f)$ values are practically equal to the imposed value for both optimization conditions. In particular, for $Z_{c2} = 50 \Omega$, both optimization conditions lead to the same results. Because practically the same values for SF were obtained for both optimization conditions, and the values for RL from Table 3 are better, the CRLH phase shifters having f_0 and $\Delta\theta$ given in Table 3 will be used in the next chapters.

For Z_{c2} equal to 50Ω and 100Ω , Fig. 6 shown the magnitude of $|S_{11}|$ after optimization, for $Z_c = 70.7 \Omega$, $\Delta f = 1.8$ GHz and $\Phi(\Delta f) = 90^\circ$, obtained with MWO, for the characteristic impedances Z'_{c1} and Z'_{c2} given in Table 1, while f_0 and $\Delta\theta$ are given in Table 3.

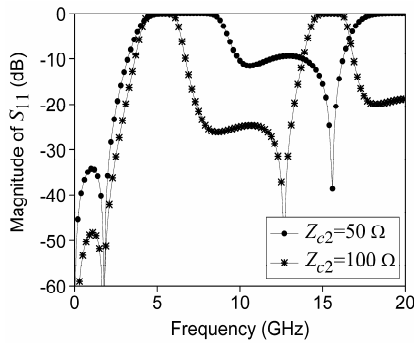


Figure 6. The magnitude of S_{11} , for the phase shifter shown in Fig. 4, when Z_{c2} is equal to 50Ω and 100Ω , obtained with MWO, after optimization (see Tables 1 and 3 for the circuit parameters).

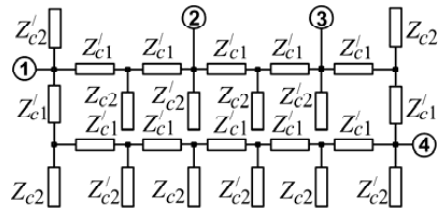


Figure 7. The configuration of CRLH based ring coupler obtained by using six CRLH based phase shifters analyzed in this paper.

3. COUPLER TOPOLOGY AND COMPARISON WITH THE TRADITIONAL RING COUPLER

A small-size ring coupler operating at the central frequency Δf may be obtained by connecting six identical CRLH based phase shifters analyzed in the previous chapter, in a configuration, as shown in Fig. 7.

If the CRLH based phase shifters are designed for $Z_c = 70.7 \Omega$

Table 4. The maximum differences between the results obtained for the CRLH based ring coupler and the traditional ring coupler, related to the last ones, for a frequency bandwidth from 1.7 GHz to 1.9 GHz.

	$Z_{c2} = 50 \Omega$	$Z_{c2} = 100 \Omega$
$ S_{21} $ (%)	0.5	0.4
$ S_{41} $ (%)	0.36	0.3
$ S_{43} $ (%)	0.43	0.33
$ S_{23} $ (%)	0.38	0.3
$ S_{31} $ (%)	2.1	2.6
$ S_{13} $ (%)	2.1	2.6
$ S_{11} $ (%)	2.4	2.1
$ S_{33} $ (%)	3.1	1.7
Phase (S_{21}/S_{41})(%)	0.14	0.16
Phase (S_{43}/S_{23})(%)	7.7	8.4

and $\Phi(\Delta f) = 90^\circ$, 3-dB ring couplers are obtained. For this case, the parameters of the CRLH based phase shifters are given in Table 1 (for Z_{c1}' and Z_{c2}') and Table 3 (for f_0 and $\Delta\theta$). The characteristics of the 3-dB traditional ring coupler and 3-dB CRLH based ring couplers designed for $Z_{c2} = 50 \Omega$ and $Z_{c2} = 100 \Omega$, have been compared by analyzing them using MWO.

The simulation results for the magnitudes of the scattering parameters and the phase shift differences are shown in Fig. 8. A good agreement between the performances of the traditional and CRLH based ring couplers may be observed.

The maximum differences between the results obtained for the CRLH based ring couplers and the traditional ring coupler, related to the last ones, for a frequency bandwidth from 1.7 GHz to 1.9 GHz, are presented in Table 4.

In the same frequency bandwidth, from Table 4, very small

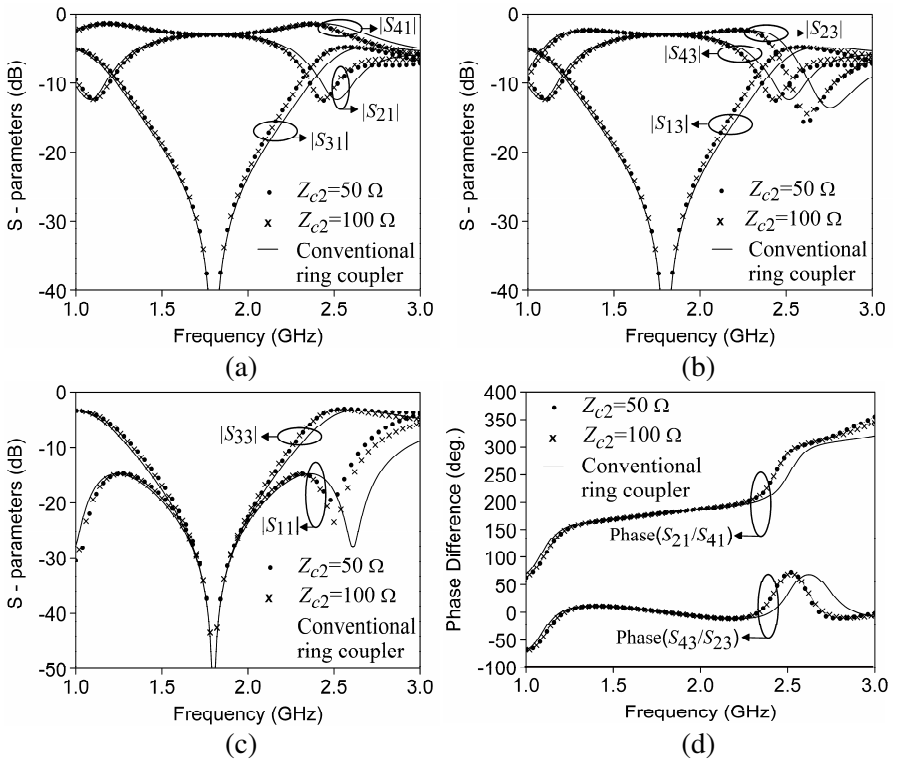


Figure 8. Simulated magnitudes of (a)–(c) the scattering parameters and simulated phase shift differences, for the traditional and CRLH based 3-dB ring couplers.

differences may be also observed between the results obtained for the CRLH based ring couplers, designed for $Z_{c2} = 50\ \Omega$ and $Z_{c2} = 100\ \Omega$. For any other value of Z_{c2} between $50\ \Omega$ and $100\ \Omega$, practically the same results are expected to be obtained between 1.7 GHz and 1.9 GHz, where the comparison has been made.

4. ELECTROMAGNETIC SIMULATION AND EXPERIMENTAL RESULTS

The layout for the 3-dB CRLH based ring coupler with $Z_{c2} = 50\ \Omega$ has been designed and fabricated with microstrip lines, for RT/duroid 5870 of 1.575 mm thickness as substrate. The photo of the fabricated circuit is shown in Fig. 9.

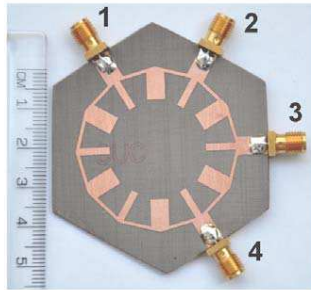


Figure 9. Photo of the fully-distributed CRLH based ring coupler.

The coupler layout has been analyzed numerically using the electromagnetic (EM) analysis capabilities from IE3D — Zeland.

Experimental results have been also obtained, using Anritsu MS2026C two-port Vector Network Analyzer (VNA). The coupler being a four-port circuit, a few sets of two-port measurements have been performed, passing the two VNA ports over the coupler ports, while the remaining two ports were matched using $50\ \Omega$ loads. The experimental results and the results obtained by EM simulation are shown in Fig. 10, for the magnitude of the scattering parameters and for the phase shift differences. A very good agreement between them is observed for the magnitudes of the scattering parameters, as well as for the phase differences between the outputs. Into the frequency bandwidth from 1.7 GHz to 1.9 GHz, these differences are less than 0.3 dB, for $|S_{21}|$, $|S_{41}|$, $|S_{23}|$ and $|S_{43}|$, less than 2 dB for $|S_{31}|$ and $|S_{13}|$, while for $|S_{11}|$ and $|S_{33}|$ these are less than 4 dB. Also, the differences for Phase (S_{21}/S_{41}) and Phase (S_{43}/S_{23}) are less than 0.5° and 1.5° , respectively.

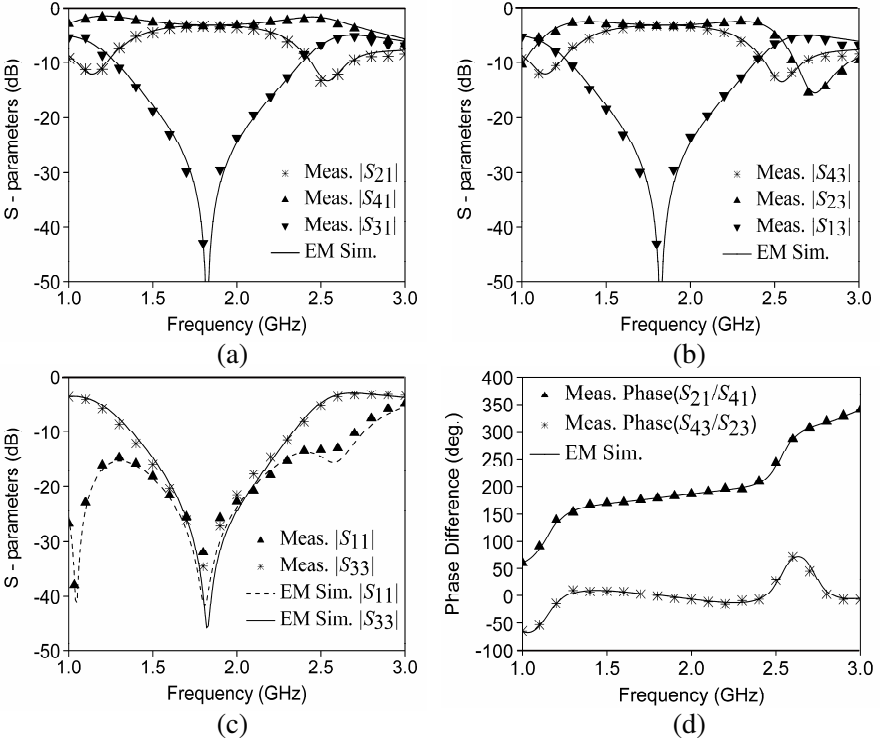


Figure 10. Simulated and experimental magnitudes of (a)–(c) the scattering parameters and (d) phase shift differences, for the CRLH based 3-dB coupler.

From the experimental data, into the same frequency bandwidth, $|S_{21}|$, $|S_{43}|$, $|S_{41}|$ and $|S_{23}|$ are within -3 ± 0.3 dB, $|S_{31}|$ and $|S_{13}|$ are smaller than -29.5 dB, while $|S_{11}|$ and $|S_{33}|$ are smaller than -25.5 dB. Also, the $\text{Phase}(S_{21}/S_{41})$ is between 175.8° and 182.9° , while the $\text{Phase}(S_{43}/S_{23})$ is between 2.9° and -4.2° .

Compared to the traditional ring coupler, the printed area of the fabricated coupler is 49% smaller.

5. CONCLUSIONS

An accurate design method for a miniaturized configuration of the ring coupler consisting of open stubs on the inside of the ring has been proposed. In comparison to other design method proposed in the literature, in the proposed design method, the characteristic

impedances of the open stubs have not the same value, in consequence, the coupler configuration may be optimized easier. For this coupler topology it has been shown that the phase shifters between the coupler arms may be seen as consisting of CRLH structures.

For the CRLH based shifter, it is demonstrated the possibility to reduce its lengths by a scaling factor which is formulated in terms of the design parameters. Also, the possibility to use the CRLH based shifter for dual-band or multi-band applications is also emphasized for the future research. In this paper, focusing on the miniaturization applications, ring couplers based on the CRLH phase shifters are designed and compared to the traditional ring coupler topology, showing that practically the same characteristics are obtained for a 10% frequency bandwidth. A CRLH based ring coupler was designed and fabricated, a printed area reduction of 49% comparing to the traditional ring coupler being obtained. The fabricated coupler has been also tested experimentally. A very good agreement between the experimental results and those predicted by electromagnetic simulation has been obtained.

ACKNOWLEDGMENT

The authors wish to acknowledge physicist Florin Craciunoiu from the Institute of Microtechnologies-Bucharest for his support concerning the circuit fabrication.

REFERENCES

1. Pon, C. Y., "Hybrid-ring directional coupler for arbitrary power divisions," *IRE Trans. Microwave Theory and Techniques*, Vol. 9, 529–535, Nov. 1961.
2. Kim, D. I. and G. S. Yang, "Design of new hybrid-ring directional coupler using $\lambda/8$ or $\lambda/6$ sections," *IEEE Trans. on Microwave Theory and Techniques*, Vol. 39, 1179–1184, Oct. 1991.
3. Coupez, J. P., A. Peden, and C. Person, "Analysis and design of ultra miniature hybrid ring directional coupler," *Proc. 22nd European Microwave Conf.*, Vol. 1, 443–447, Helsinki, Finland, 1992.
4. Murgulescu, M. H., M. Moisan, P. Legaud, E. Penard, and I. Zaquine, "New wideband, $0.67\lambda_g$ circumference 180° hybrid ring coupler," *Electronics Letters*, Vol. 30, No. 4, 299–300, Feb. 1994.
5. Murgulescu, M. H., E. Penard, and I. Zaquine, "Design formulas

- for generalized 180° hybrid ring couplers,” *Electronics Letters*, Vol. 30, No. 7, 573–574, 1994.
6. Wang, T. and K. Wu, “Size-reduction and band-broadening design technique of uniplanar hybrid ring coupler using phase inverter for M(H)MIC’s,” *IEEE Trans. on Microwave Theory and Techniques*, Vol. 47, 198–206, Feb. 1999.
 7. Chi, P. L., “Miniaturized ring coupler with arbitrary power divisions based on the composite right/left-handed transmission lines,” *IEEE Microwave and Wireless Components Letters*, Vol. 22, 170–172, Apr. 2012.
 8. Okabe, H., C. Caloz, and T. Itoh, “A compact enhanced-bandwidth hybrid ring using an artificial lumped-element left-handed transmission-line section,” *IEEE Trans. on Microwave Theory and Techniques*, Vol. 52, 798–804, Mar. 2004.
 9. Fouda, A. E., A. M. E. Safwat, and H. El-Hennawy, “On the applications of the coupled-line composite right/left-handed unit cell,” *IEEE Trans. on Microwave Theory and Techniques*, Vol. 58, 1584–1591, Jun. 2010.
 10. Chuang, M. L., “Miniaturized ring coupler of arbitrary reduced size,” *IEEE Microwave and Wireless Components Letters*, Vol. 15, 16–18, Jan. 2005.
 11. Simion, S., “Small-size ring coupler design method based on fully distributed composite right/left handed approach,” *Electronics Letters*, Vol. 48, No. 23, 1481–1483, Nov. 2012.
 12. Kim, D. I. and Y. Naito, “Broad-band design of improved hybrid-ring 3-dB directional couplers,” *IEEE Trans. on Microwave Theory and Techniques*, Vol. 30, No. 11, 2040–2046, Nov. 1982.
 13. Ho, C. H., L. Fan, and K. Chang, “Broadband uniplanar hybrid ring coupler,” *Electronics Letters*, Vol. 29, No. 1, 44–45, Jan. 1993.
 14. Chi, P. L. and T. Itoh, “Miniaturized dual-band directional couplers using composite right/left-handed transmission structures and their applications in beam pattern diversity systems,” *IEEE Trans. on Microwave Theory and Techniques*, Vol. 57, 1207–1215, May 2009.
 15. Pozar, M. D., *Microwave Engineering*, 3rd Edition, Chapter 8, Wiley, New York, 2005.